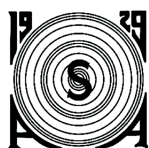

euronoise

www.acoustics08-paris.org

Stroboscopic White Light Interferometry for Dynamic Characterization of Capacitive Pressure Sensors

Ivan Kassamakov[a], Kalle Hanhijärvi[a], Juha Aaltonen[a], Lauri Sainiemi[b], Kestutis Grigoras[b], Sami Franssila[b] and Edward Hæggström[a]

[a]Electronics Research Unit, University of Helsinki, P.O.Box 64 (Gustaf Hällströmin katu 2), FIN-00014 Helsinki, Finland
[b]Micro and Nanosciences Laboratory, Helsinki University of Technology, P.O.Box 3500, FI-02015 TKK, Finland
kalle.hanhijarvi@helsinki.fi

Scanning white light interferometry (SWLI) is a well-established method for accurate static out-of-plane 3-D profiling of micromechanical devices. Periodic displacements can be measured using a stroboscopic illumination synchronized to an arbitrary phase angle of the sample oscillation. We modified an existing SWLI setup for dynamic characterization. A two-channel function generator drives the sample and the stroboscopic illumination, and controls the inter-channel phase. A phosphorous white light LED is used as light source. Currently our shortest stroboscopic pulse is 50 ns. We measured the out-of-plane displacement of a thermal microbridge fabricated on SOI wafer with an accuracy of 20 nm. The microbridge was driven with sinusoidal and square wave signals (1 Hz - 960 Hz). The stroboscopic duty cycles were 0.1% - 5%. We also characterize the vibration modes of a capacitive pressure sensor membrane at 173.93 kHz. Stroboscopic SWLI has been found useful in nanoscale profile measurements of periodic oscillations. Capability of dynamic out-of-plane deflection measurement was demonstrated at low (100 Hz) and high (100 kHz) frequencies.

1 Introduction

Scanning white light interferometry (SWLI) is a widely applied and accurate method for *static* 3D profiling of microelectromechanical systems (MEMS) devices [1, 2, 3]. A low coherence light source, such as halogen lamp or a light emitting diode (LED) produces a spatially localized interference. Consequently unlike laser-based approaches, SWLI does not suffer from phase ambiguity. To improve MEMS manufacturing methods and end-product reliability, mechanical properties of such devices (e.g. thermal expansion, spatial modes) needs to determined during operation. SWLI can be used for *dynamic* device characterization of periodically oscillating samples, if a stroboscopic illumination synchronized with sample operation is employed [4, 5, 6]. The sample is illuminated with short light pulses produced at frequency synchronized to the sample movement. In practice, the same phase angle is illuminated at each period. If the pulse duration is short compared to the length of the driving period, the sample appears to be stationary when measured with a detector (e.g. CCD camera). Arbitrary phase angles can thus be measured by changing the relative phase difference between the illumination and sample driving signals. Dynamic device parameters (e.g. thermal expansion) can be measured, which allows verifying complex FE models. Commercial stroboscopic interferometers exist and provide a robust and accurate method for dynamic characterization of out-of-plane oscillations in MEMS. Moreover, since SWLI is a full-field method, it provides advantages over point-measurement-based approaches, such as laser doppler vibrometry (LDV). Stroboscopic SWLI offers faster measurement time and wider dynamic range than LDV measurement.

2 Theory and background

2.1 Scanning white light interferometry

In a typical SWLI measurement the optical path difference (OPD) between sample surface and reference mirror is modulated by displacing the interferometric objective (e.g. Michelson or Mirau) with a piezoelectric scanner. The light intensity is sampled pixel-by-pixel with a CCD-camera at given OPD ($\lambda_m/8$, where λ_m is the mean wavelength of the light source). The intensity as a function of arm length difference (z) is [7, 8]:

$$I = I_0 + I_R C\big(z - 2h(x,y)\big)\cos\left(\frac{4\pi}{\lambda_m} z - \alpha(x,y)\right) \quad (1)$$

where I where I_0 and I_R are the bias and reflected intensities, respectively. C is the coherence contrast or envelope of the interferogram and α is the phase change caused by reflection or transmission through the optical components. Coordinates x and y represent the position in the plane perpendicular to the scanning direction whereas h is the relative surface height. Both the envelope and cosine terms depend on the difference in arm length, and thus the relative surface height can be deduced from either one [7, 8]. The method applied here uses the peak of the envelope function, which represents the relative height of a given point. The square of the modulation function is given by the FSA algorithm [7, 8]:

$$M^2 \propto (I_2 - I_4)^2 - (I_1 - I_3)(I_3 - I_5) \quad (2)$$

where I_1 through I_5 are the recorded intensities. Moreover, I_3 represents the point for which the modulation is calculated. The other indices correspond to the respective adjacent points relative to the I_3-point. The height is calculated from the weighted fit of a Gaussian function [7, 8]:

$$z_{FSA} = 0.4\Delta\left(\frac{L_1 + 3L_2 - 3L_4 - L_5}{L_1 - L_3 + L_5}\right) \quad (3)$$

where L_1 through L_5 are the respective logarithms of the envelope contrast and Δ is the sampling interval.

2.2 Stroboscopic principle

Typical detectors used in SWLI measurements (CCD-cameras) are relatively slow (frame rates up to 1 kHz), and cannot be used in dynamic measurements as such. The scanning procedure in the SWLI measurement complicates matters further. The limitation of detector bandwidth and measurement speed can be circumvented by using stroboscopic illumination. By definition, a periodically moving surface returns to the same position after each period. If a pulsed light source is synchronized to the frequency of the illuminated sample, and if the pulse length is short compared to the oscillation period, the image appears frozen. This is due to the fact that the light pulses illuminate the same phase angle at each period of the oscillation. A relatively slow and cheap detector (CCD-camera) can therefore be used to measure dynamic profiles of periodically moving samples.

The duty cycle of the stroboscopic pulse should be short enough to properly freeze the movement. Stroboscopy-

related fringe-contrast loss has been studied by de Groot [9] according to whom a condition can be written to ensure that the measurement error from the averaging effect of stroboscopic illumination is kept below 2 nm. If the duty cycle is below 10% and if the product of the peak-to-valley oscillation amplitude and the duty cycle is less than the mean wavelength divided by 25, the condition is fulfilled. A lower limit for the duration is set by the required intensity SNR.

3 Experimental setup and samples

3.1 Stroboscopic interferometer

We have built a SWLI system based on an in-house designed bridge-frame construction. The bridge is stable and acts as a vibration damper. The interferometric objective is an infinity corrected either Michelson (Nikon 5x) or Mirau type (Nikon 10x). Additional focusing and collimating optics are used to provide parallel light. The OPD modulation is achieved with a piezoelectric scanner (PI P-725) attached to the objective. Intensity data are recorded with a 8-bit high speed monochrome progressive scan CCD-camera (Pulnix TM-6740GE). Piezo control and image acquisition are controlled by custom programmed measurement software running on a PC. The stroboscopic system (Fig. 1) consists of a two-channel arbitrary function generator (Tektronix AFG3252), which provides signals for sample and illumination. A high intensity white color LED (Luxeon LXHL-MW1D) is used as a light source [10]. The LED is connected to the signal generator through a custom designed pulse amplifier. A momentary current of 350 mA is used to ensure sufficient level of intensity during the measurement. A four channel oscilloscope (Tektronix TDS2024B) visualizes the stroboscopic signals.

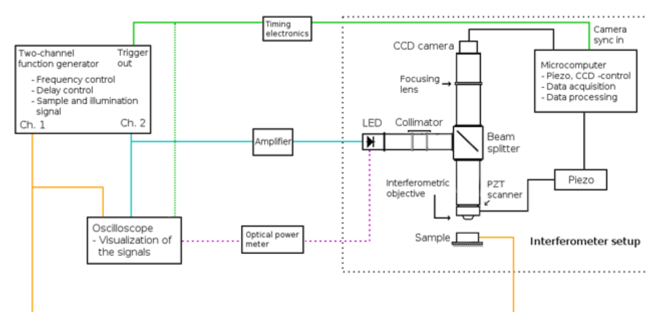

Fig. 1 Schematic of the stroboscopic interferometer setup

The camera exposure is triggered through a frequency divider circuit to eliminate flickering at frequencies close to the framerate. At high frequencies flickering does not pose a significant problem and can be ignored.

The frequency bandwidth of a stroboscopic system depends on its capability to produce short pulses. Currently the amplifier limits the pulse duration to 50 ns.

3.2 Laser Doppler Vibrometer

As a reference measurement the pressure sensor was measured with a commercial Laser Doppler Vibrometer (Polytec OFV-3001) equipped with an ultrasonic displacement decoder (Polytec OVD-30). The frequency bandwidth of the LDV is limited at the low end to 50 kHz, and so the microbridges could not be measured with it.

3.3 Thermal microbridges

Deflection of a thermal silicon microbridge actuator was studied during operation. The measurements were done using a microbridge that was 400 µm long, 20 µm wide, and 4 µm thick. The bridge was clamped from both ends to 1 mm wide square shaped anchor areas (Fig. 2). The anchor areas carried aluminum electrical contact pads. The periodic thermal expansion was induced by applying a sinusoidal voltage (0 V – 4 V, 120 Hz – 600 Hz) to the aluminum pads. This voltage across the bridge heated it due to Joule heating.

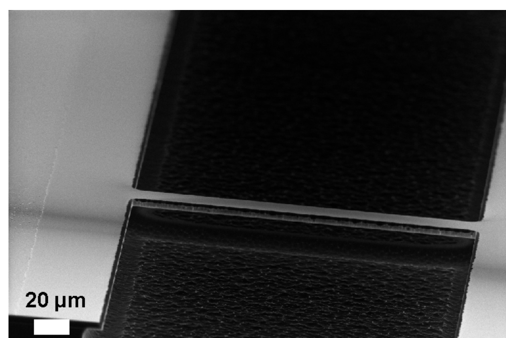

Fig. 2 Scanning electron microscope image of fabricated silicon microbridge.

The detailed fabrication process of the microbridge actuators is discussed elsewhere [11]. Shortly, the microbridges were fabricated on a silicon-on-insulator (SOI) wafer that featured a 4 µm thick highly doped device layer, 200 nm thick buried oxide (BOX) layer, and 380 µm thick handle wafer. First, an aluminum layer was sputtered onto the wafer and patterned to create square shaped electrical contact pads. The second lithography step and deep reactive ion etching of the device layer and the BOX defined the lateral dimensions of the actuator. The thickness of the bridges was defined by the device layer thickness. The bridge sidewalls were subsequently protected using plasma enhanced chemical vapor deposited silicon dioxide, after which the bridge was released from the handle wafer using isotropic plasma etching of silicon. Finally, the protecting silicon dioxide layers were removed in hydrofluoric acid. The processed wafer contained several different bridge dimensions.

3.4 Capacitive pressure sensors

The capacitive piston mode pressure sensor utilizes a released electrode in the device layer of SOI (Silicon-On-Insulator) as the moving electrode coupling to the pressure (Fig. 4).

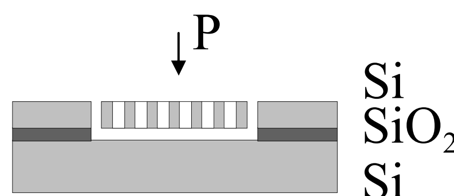

Fig. 3 Cross-sectional view of the sensor.

The lower electrode of the sensor is fixed whereas the elastically supported upper electrode is able to move due to the pressure difference between the exterior of the sensor and the internal vacuum reference chamber.

4 Results

4.1 Thermal microbridges

The out-of-plane deflection of the thermal microbridges was measured with a sinusoidal excitation (4V amplitude, 4V DC offset, 120 Hz), which resulted in periodic expansion of the sample. The maximum measured bridge deflectction (Figs. 4 and 5) at 90° phase angle was (3.20 ± 0.02) µm, which agrees with simulated predictions.

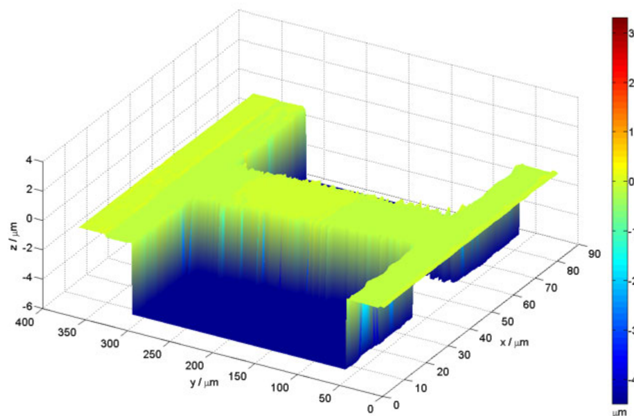

Fig. 4 Measured out-of-plane deflection of a periodical thermal expansion of a microbridge; 0° phase angle; color bar units are in micrometers

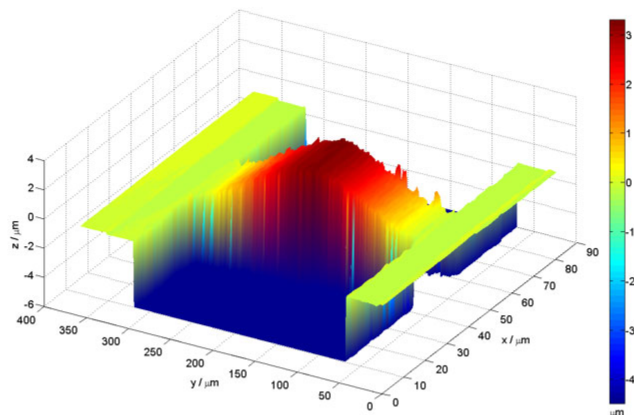

Fig. 5 Measured out-of-plane deflection of a periodical thermal expansion of a microbridge; 90° phase angle; color bar units are in micrometers

4.2 Capacitive pressure sensors

The out-of-plane movement of the pressure sensor was measured with a LDV from the middle part of the membrane structure. The frequency of the maximum peak-to-peak displacement was measured to be 173.93 kHz. This frequency was employed in the consecutive SWLI measurements. At this frequency the LDV measurement showed a peak-to-peak displacement of (108 ± 2) nm (Fig. 6). A 10 V DC bias of and a 3V amplitude sinusoidal signal with were applied to the device.

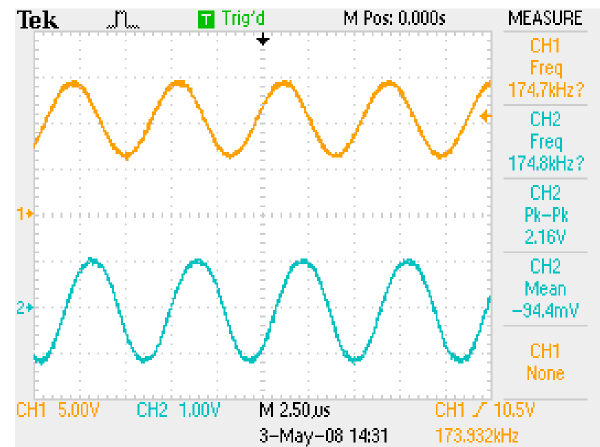

Fig. 6 Oscilloscope screen dump from the LDV measurement; Top: Drive voltage; Bottom: Signal from displacement decoder (50 nm/V)

The deflected profile of the pressure sensor membrane was measured from 0° to 360° phase angle at 10° increments. Increase in drive voltage resulted in downward deflection relative to the sensor frame (Figs. 7 and 8). Line profile measured across the sensor reveals uneven bending of the membrane (Fig. 9).

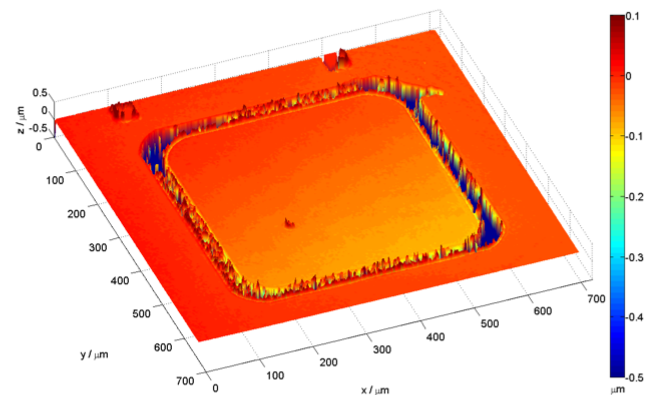

Fig. 7 Measured out-of-plane deflection of the pressure sensor; 0° phase angle

Average deflection calculated from the middle part of the membrane (50x50 µm square) changes in a sinusoidal manner as a function of phase angle (Fig. 10).

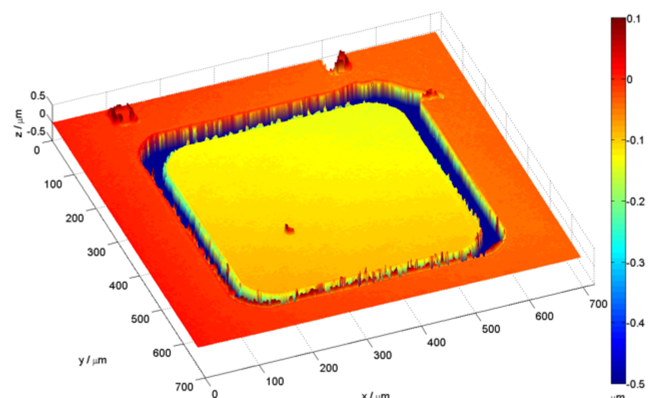

Fig. 8 Measured out-of-plane deflection of the pressure sensor; 100° phase angle

The peak-to-peak movement measured from the average bending was (110 ± 15) nm, which agrees with the LDV measurement. The deflection was measured from the approximate centre part with the LDV, which accounts for the systematic difference between the instruments.

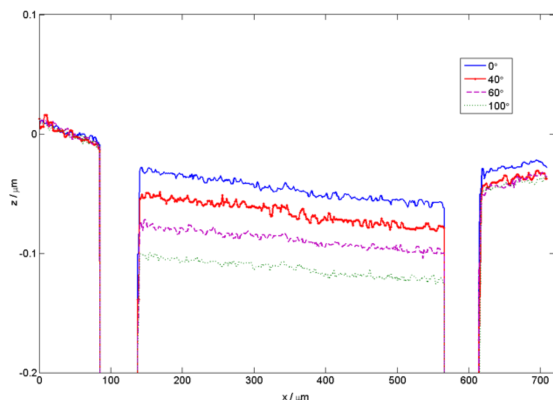

Fig. 9 Line profile measured across the sensor as a function of phase angle

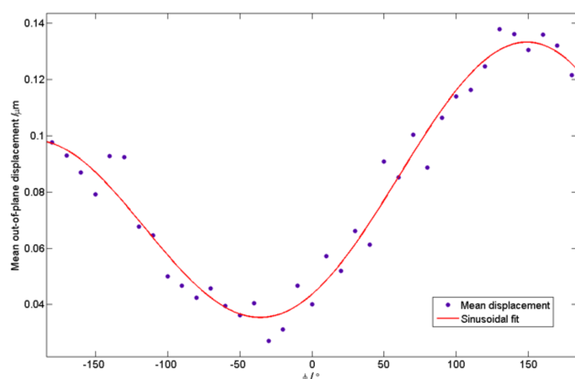

Fig. 10 Average membrane displacement as a function of duty cycle

5 Conclusion

From the results presented above, it can be concluded that stroboscopic SWLI can be used for full-field characterization of out-of-plane deflections in MEMS devices. Capability to measure periodic oscillation was demonstrated both at low (100 Hz) and high (100 kHz) frequencies. The stroboscopic system could in principle be used with frequencies up to 1 MHz. Resolution in z-direction depends largely on background vibrations, -here measured to be 20 nm. The averaging effect of the stroboscopic measurement is negligible if the duty cycle is short (3%) compared to the length of the driving period. For high frequency measurements, the results were validated by comparison to results obtained with a commercial LDV system.

Acknowledgments

Anu Kärkkäinen and Teuvo Sillanpää from VTT Technical Research Centre of Finland for providing us with the samples.

References

[1] T. Dresel, G. Häusler, H. Venzke, "Three-dimensional sensing of rough surfaces by coherence radar," Appl. Opt., 21(7), 919-925 (1992)

[2] G.S. Kino, S.S.C. Chim, "Mirau correlation microscope," Appl. Opt., 29(26), 3775-3783 (1990)

[3] P. de Groot, L. Deck, "Surface Profiling by Analysis of White-light Interferograms in the Spatial Frequency Domain," J. Mod. Opt., 42(2), 389-401 (1995)

[4] S. Petitgrand, R. Yahiaoui, K. Danaie, A. Bosseboeuf, J.P. Gilles, "3D measurement of micromechanical devices vibration mode shapes with a stroboscopic interferometric microscope," Opt. Lasers Eng., 36(2), 77-101 (2001)

[5] L.A.J. Davis, D.R. Billson, D.A. Hutchins, R.A. Noble, "Visualizing acoustic displacements of capacitive micromachined transducers using an interferometric microscope," Acoust. Res. Lett. Online-ARLO, 6(2) 75-79 (2005)

[6] C. Rembe, R. Kant, R.S. Muller, "Optical Measurement Methods to Study Dynamic Behavior in MEMS," Proc. SPIE 4400, 127-137 (2001)

[7] K.G. Larkin, "Efficient nonlinear algorithm for envelope detection in white light interferometry," J. Opt. Soc. Am. A-Opt. Image Sci. Vis., 13(4) 832-843 (1996)

[8] A. Harasaki, J. Schmit, J.C. Wyant, "Improved vertical-scanning interferometry," Appl. Opt., 39(13) 2107-2115 (2000)

[9] P. de Groot, "Stroboscopic white-light interference microscopy,", Appl. Opt., 45(23), 5840-5844 (2006)

[10] K. Hanhijärvi, J. Aaltonen, I. Kassamakov, E. Hæggström, "3-D Dynamic Profilometry of M(O)EMS Using Stroboscopic Scanning White Light Interferometry" Report Series in Physics, HU-P-267, Proc. of the XLI Annual Conference of the Finnish Physical Society (2007)

[11] L. Sainiemi, K. Grigoras, I. Kassamakov, K. Hanhijärvi, J. Aaltonen, J. Fan, V. Saarela, S. Franssila, "Fabrication and electrical, mechanical and optical characterization of SOI thermal microbridge actuators", submitted to Sens. Actuator A-Phys